RECENT ADVANCES IN PHYSICAL MODELING WITH K- AND W-TECHNIQUES

Matti Karjalainen, Jyri Pakarinen, Cumhur Erkut, Paulo A. A. Esquef, and *Vesa Välimäki*

Helsinki University of Technology
Laboratory of Acoustics and Audio Signal Processing
{firstname.lastname}@hut.fi

ABSTRACT

Physical (or physics-based) modeling of musical instruments is one of the main research fields in computer music. A basic question, with increasing research interest recently, is to understand how different discrete-time modeling paradigms are interrelated and can be combined, whereby wave modeling with wave quantities (W-methods) and Kirchhoff quantities (K-methods) can be understood in the same theoretical framework. This paper presents recent results from the HUT Sound Source Modeling group, both in the form of theoretical discussions and by examples of K- vs. W-modeling in sound synthesis of musical instruments.

1. INTRODUCTION

Real-world systems of interest in acoustics and computer music are typically continuous in time and space, and therefore their dynamic behavior is inherently described by partial differential equations [1]. Computer-based modeling and simulation of them requires, however, discretization of the underlying PDEs, which in a general case corresponds to the continuous analog system only when sample rate approaches infinity, i.e., temporal and spatial sample intervals are made infinitesimally small.

In this paper we discuss several discrete-time modeling paradigms, particularly the *digital waveguides* (DWGs), *wave digital filters* (WDFs), and *finite difference time domain schemes* (FDTDs). Their properties are compared and their mixing to hybrid modeling techniques are probed further from previous studies. Two cases (wave digital bell and distributed nonlinearity by FDTDs) are used to characterize realization principles.

1.1. General viewpoints

Discretization in time and space leads to interesting and difficult problems that are not found in the ordinary continuous case. Particularly when systems are *simulated* or *synthesized* efficiently in the time domain by discrete techniques, in contrast to being *solved* from equations, the question of *localized discretization* (blockwise construction of models through interconnection of elements) and consistent *scheduling* (ordering of operations) are of major importance.

In the analog world we may in the limit assume arbitrarily short (infinitesimal) delays between spatial points of interest, and the order of events follows the causality principle of physics. In the discrete-time world, however, a single sample period is the shortest possible non-zero time interval, in which explicit two-way physical interaction can happen. This leads easily to the problem of *delay-free loops*, i.e., implicit equations where the output of an operation needs an input value that may be dependent on the output value not yet known. Particularly with nonlinear elements this is a fundamental problem [2], in addition to aliasing.

It is now well-known that the delay-free loop problem is easier to overcome if computations are formulated by wave components instead of ordinary physical quantities [3]. Referring to electric circuits, the latter ones are often called the *Kirchhoff quantities*, in contrast to *wave quantities*. Using dual K-variables (K for Kirchhoff), such as voltage and current or force and velocity, is very intuitive for circuits and their mechanical equivalents, but in the discrete methodology they are not as easy to use. K-elements formulated as transfer functions between dual K-variables cannot form circuits and networks directly, but they in general must be converted into wave-based formulation, in order to compute them by explicit relations as local interactions. This is different from solving system equations [1] which permits global interactions.

This paper is organized as follows. Section 2 presents a condensed overview of the physical modeling paradigms of interest in this study. In Section 3 we investigate the interrelations of these paradigms, followed by a case study of a wave digital bell model in Section 4. In Section 5, distributed nonlinear W-modeling is investigated, followed by a summary of the paper.

2. PARADIGMS OF DISCRETE-TIME MODELING

A short characterization of different physical modeling paradigms is presented in this Section, including digital waveguides, wave digital filters, finite difference time domain schemes, and modal decomposition.

2.1. Digital waveguides

Digital waveguide modeling is based on the fact that wave propagation in a medium can be simply and efficiently simulated by two delay lines [4], one for each directional wave component. This is closely related to the d'Alembert solution of the wave equation. By proper discretization in time and space the delay lines can be updated simply by

$$\vec{y}_{k,n+1} = \vec{y}_{k-1,n} \quad \text{and} \quad \overleftarrow{y}_{k,n+1} = \overleftarrow{y}_{k+1,n} \qquad (1)$$

where arrows denote the right- and left-traveling components of the total waveform, and indices k and n refer to discrete position and time, respectively. Lowpass and allpass filters can be cascaded with delay elements to simulate damping and dispersion. Delay sequences between points of signal observation (output) and feed-in (input) can be consolidated into subsystems that are computationally highly efficient [4].

In addition to delays we need connecting junctions that fullfil physical continuity constraints, i.e., the Kirchhoff rules. For a parallel junction of acoustic components we may write:

[1] Time-domain simulation can also be based on solving global equations for each time step, but that tends to be highly inefficient compared to block-based simulation by localized interactions.

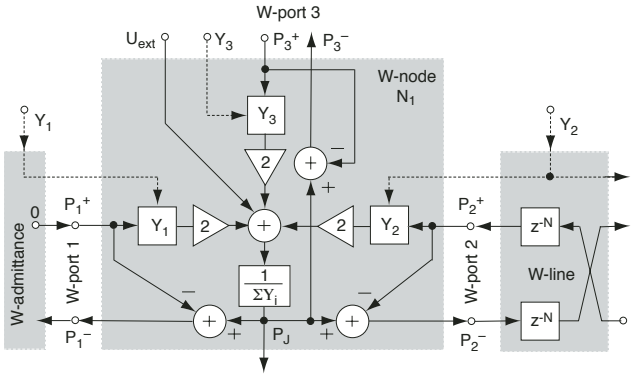

Figure 1: *A 3-port parallel scattering junction for acoustic pressure waves. Port 1 (left) is terminated by admittance Y_1, port 2 (right) is connected to a delay-line, and port 3 (top) is not connected.*

$$P_1 = P_2 = \ldots = P_N = P_\mathrm{J} \tag{2}$$

$$U_1 + U_2 + \ldots + U_N + U_\mathrm{ext} = 0 \tag{3}$$

where P_i are pressure and U_i volume velocities at the ports of the junction, P_J is the common pressure of coupled branches and U_ext is an external volume velocity to the junction. When port pressures are represented by incoming wave components P_i^+ and outgoing wave components P_i^-, admittances attached to each port by Y_i, and

$$P_i = P_i^+ + P_i^- \quad \text{and} \quad U_i^+ = Y_i P_i^+ \tag{4}$$

the junction pressure P_J can be obtained as:

$$P_\mathrm{J} = \frac{1}{Y_\mathrm{tot}}(U_\mathrm{ext} + 2\sum_{i=0}^{N-1} Y_i P_i^+) \tag{5}$$

where $Y_\mathrm{tot} = \sum_{i=0}^{N-1} Y_i$ is the sum of all admittances to the junction. Outgoing (scattered) pressure waves, obtained from Eq. (4), are then $P_i^- = P_\mathrm{J} - P_i^+$. Figure 1 depicts this as a signal flow diagram for the computation of such a scattering junction.

The same diagram can be applied to a series connection and volume velocity waves so that pressures and volume velocities are interchanged and admittances are replaced by impedances.

2.2. Wave digital filters

Wave digital filters (WDFs) are models that were originally developed for discrete-time simulation of lumped element circuits and systems as they were known from the analog electric domain [3]. The close relationship between them and digital waveguides is well known [4, 5]. While DWGs emphasize delays and wave propagation, WDFs have emphasis on lumped element modeling. However, both are capable to both types, and actually they are compatible and complementary approaches to wave-based modeling.

The WDF formalism is based on a notation of ('voltage') waves a and b as

$$\begin{cases} a = V + RI \\ b = V - RI \end{cases} \quad \leftrightarrow \quad \begin{cases} V = (a+b)/2 \\ I = (a-b)/2R \end{cases} \tag{6}$$

where a is in-coming and b is out-going wave in a port, V is voltage and I is current as Kirchhoff variables, and R is port resistance (reference resistance). In Fig. 2 a model for series connection of

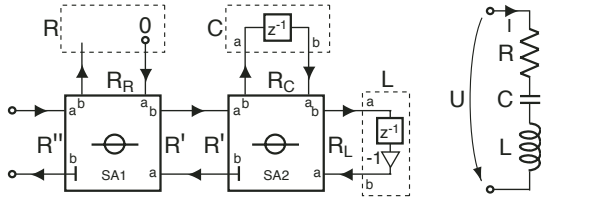

Figure 2: *(Left) A WDF series connection of resistor (R), capacitor (C), and inductor (L) constructed by two three-port series adaptors (SA1 and SA2). (Right) Equivalent analog circuit.*

inductor L, capacitor C, and resistor R is depicted. It is constructed by two three-port *series adaptors* (SA1 and SA2) that implement wave scattering according to Kirchhoff laws. The implementation of the R, C, and L components is shown. Delay-free loops are avoided by the structure of the components and by impedance-matched reflection free ports denoted by $-|$ in the adaptors [3].

In a closer comparison of DWGs (Eq. (3-5) and Fig. 1) and WDFs (Eq. (6) and Fig. 2) we can see that through acoustical-to-electrical analogies $P_i^+ = a$, $P_i^- = b$, $P_i = V$, $U_i = I$, and $1/Y_i = R$, for the DWG we get

$$\begin{cases} a = (V + RI)/2 \\ b = (V - RI)/2 \end{cases} \quad \leftrightarrow \quad \begin{cases} V = (a+b) \\ I = (a-b)/R \end{cases} \tag{7}$$

which shows a difference in scaling compared to the WDF convention in (6). In fact we may select the scaling quite freely if we are interested just to get physically proper values of the Kirchhoff quantities V and I. One useful convention is to apply *power-normalized waves* [3, 4] by

$$\begin{cases} a = (V + RI)/2\sqrt{R} \\ b = (V - RI)/2\sqrt{R} \end{cases} \quad \leftrightarrow \quad \begin{cases} V = (a+b)\sqrt{R} \\ I = (a-b)/\sqrt{R} \end{cases} \tag{8}$$

which have the favourable property that port power $P = V \cdot I = a^2 - b^2$ is independent of changes in R.

If the port admittances/impedances in DWG junctions are real-valued, the DWG junctions and WDF adaptors implement the same computation of K-variables, thus they are just two slightly different formulations of the same W-modeling principle. The WDF theory supports combinations of parallel and series connections (typically by 2- and 3-port adaptors) using reflection-free ports as in Fig. 2. The WDF theory includes a set of lumped one- and two-ports, and it is generalized also to multidimensional modeling [3].

2.3. Finite difference models

Finite difference approximation is a popular method of numerical integration of partial differential equations [6]. In physical modeling it is used particularly for multidimensional mesh structures [5] but also for example in string modeling [7].

Second order differences applied to the wave equation with a proper space and time discretization yield a simple recursion formula

$$y_{k,n+1} = y_{k-1,n} + y_{k+1,n} - y_{k,n-1} \tag{9}$$

for the computation of an FDTD node variable for a 1-D FDTD structure, whereby indices k and n refer to spatial and temporal indices, respectively [4]. In [8] we have derived an extension of the scheme that allows FDTD structures with arbitrary connection admittanced to be formed, see Fig. 3, in a way very similar to the

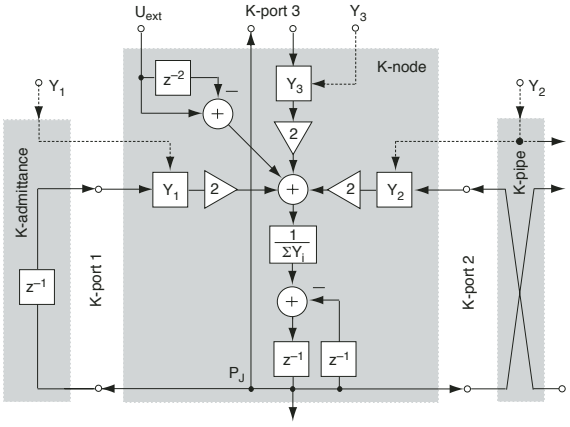

Figure 3: *A three-port parallel connection of FDTD type, corresponding to the DWG in Fig. 1.*

DWG diagram in Fig. 1. The generalized recursion formulation for the structure (without excitation U_{ext}) becomes

$$P_{\text{J},n+1} = \frac{2}{Y_{\text{tot}}} \sum_{i=0}^{N-1} Y_i P_{i,n} - P_{\text{J},n-1} \qquad (10)$$

Notice that volume velocity excitation U_{ext} must be fed through a simple FIR filter $H(z) = 1 - z^{-2}$. The equivalence of the DWG in Fig. 1 and the FDTD structure in Fig. 3 has been proven in [8] and details of their relations will be discussed in Section 3.1.

2.4. Modal decomposition techniques

While the DWG, WDF, and FDTD methods above are explicit time-domain simulation techniques, the *modal decomposition* methods rely on frequency-domain formulations of systems under study. They decompose the behavior of a system into decaying exponentials, whereby oscillatory components represent eigenmodes of the system. Modal decomposition methods include the traditional *modal synthesis* [9] and a newer approach called *functional transformation method* (FTM) [10]. In Section 4 we will study semiphysical modeling of bells based on a modal decomposition paradigm.

3. K- VS. W-MODELING

As mentioned above, it is well known that block-based modeling with K-methods is difficult or impossible due to the delay-free loop problem. There are special techniques, however, to use K-modeling, and the combination of K- and W-blocks is of particular interest. In this Section we discuss some related questions.

3.1. Comparison of DWG vs. FDTD models

In [8] we have presented a careful analysis of DWGs and FDTDs as shown in Figs. 1 and 3, by proving their functional equivalence in processing related K-variables. There are, however, a couple of special questions related to the equivalence need to be addressed.

The first one deals with the 'sporadic' or 'spurious' oscillations that easily appear in the FDTD structure but not in DWGs. The potential instabilities in FDTD are due to its inherent dual-delay feedback, see the bottom part of Fig. 3. This creates poles at DC and Nyquist frequency that need to be counteracted by the

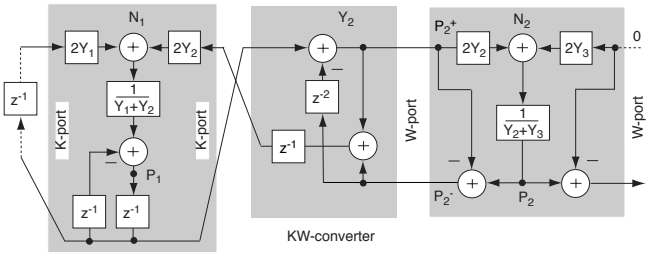

Figure 4: *KW-converter for mixed modeling with FDTDs (left-hand side) and DWGs (right-hand side).*

term $H(z) = 1 - z^{-2}$ when feeding external excitation U_{ext}. This pole cancellation means lack of numerical robustness close to these frequencies. Without this term an impulse fed to the junction results in continuous Nyquist frequency oscillation plus step function propagating from the junction in an FDTD array, which means unbound generation of energy, thus being nonphysical in the sense of passive systems.

One may ask if the instability is possible in a DWG. It is only possible if the junction is fed through the inverse of $H(z) = 1 - z^{-2}$, i.e., through $H(z) = 1/(1 - z^{-2})$, which works as an external source to make continuous energy generation.

Another special case is the inherent integration property of an FDTD structure as utilized in [7] and [11]. If only the pole at the Nyquist frequency is cancelled by feeding the FDTD junction through $H(z) = 1 + z^{-1}$, the model is inherently integrating from velocity $V(z)$ to displacement $Y(z)$ by $Y(z) = V(z)1/(1-z^{-1})$. This is useful for example in string modeling [11] when the desired pair of K-variables is force and displacement, instead of the 'natural' pair of force and velocity.

Now we can notice that DWGs in their basic form don't integrate. If we desire to have that property, we must use an explicit integrator, approximated by $H(z) = 1/(1 - z^{-1})$, either in feeding the input to a junction, or when taking the velocity output from a junction. By such an external element we can again make the FDTD and DWG structures fully equivalent functionally.

3.2. Compatibility of DWG vs. FDTD models

In [8] we have shown a way to construct mixed models by combining FDTD and DWG elements (thus also WDFs) through a K-to-W converter two-port, as shown in Fig. 4. The left-hand side shows an FDTD junction and the right-hand side a DWG junction. The KW-converter maps the K-variable terminals of an FDTD to a wave port of a DWG junction and the other way around.

3.3. Arbitrary impedance as a part of W-model

To derive rules for attaching an arbitrary K-defined impedance to a wave port we can write:

$$a = V + R\,I, \qquad b = V - R\,I, \quad \text{and} \quad Z = V/I \qquad (11)$$

which can be solved for $H(z)$ as a the ratio of b and a in the form

$$H(z) = \frac{b}{a} = \frac{V - RI}{V + RI} = \frac{Z - R}{Z + R} \qquad (12)$$

Now it is obvious that in general $H(z)$ includes a delay and is explicitly computable only when $\hat{z}(n)$, the inverse Z-transform of $Z(z)$, has a delay-free component $\hat{z}(0) \neq 0$, and port resistance R is selected as $R = \hat{z}(0)$. We will next look at three common

cases of impedance $H(z)$ specification: Polynomial (FIR), rational (IIR), and a modal filterbank of second-order resonators.

FIR type impedance: When $Z(z)$ is given as a Z-domain polynomial expression, i.e.,

$$Z_{\mathrm{p}}(z) = \sum_{i=0}^{N-1} q_i z^{-i} \tag{13}$$

then the a to b scattering function $H(z)$ will in a delay-containing case $R = q_0$ become

$$H_{\mathrm{p}}(z) = \frac{\sum_{i=0}^{N-1} q_i z^{-i} - R}{\sum_{i=0}^{N-1} q_i z^{-i} + R} = \frac{\sum_{i=0}^{N-2} \frac{q_{(i+1)}}{2q_0} z^{-i}}{1 + \sum_{i=1}^{N-1} \frac{q_i}{2q_0} z^{-i}} z^{-1} \tag{14}$$

which is an IIR filter cascaded with a unit delay.

IIR type impedance: When $Z(z)$ is given as a Z-domain rational expression (for simplicity numerator and denominator orders are the same), i.e.,

$$Z_{\mathrm{r}}(z) = \frac{\sum_{i=0}^{N-1} q_i z^{-i}}{\sum_{i=0}^{N-1} p_i z^{-i}} \tag{15}$$

then the delay-containing requirement for port resistance becomes $R = q_0/p_0$ and $H(z)$ according to Eq. (12) will be

$$H_{\mathrm{r}}(z) = \frac{\sum_{i=0}^{N-2} \frac{q_{i+1} - Rp_{i+1}}{2Rp_0} z^{-i}}{1 + \sum_{i=1}^{N-1} \frac{q_i + Rp_i}{2Rp_0} z^{-i}} z^{-1} \tag{16}$$

which is again an IIR filter with a cascaded unit delay.

Second order resonators: Second order resonators are of special interest because they are useful in building modal decomposition models. For example a series RLC-resonator having poles at DC and Nyquist frequency can be simulated by

$$Z_{\mathrm{s}} = K \frac{1 + q_1 z^{-1} + q_2 z^{-2}}{1 - z^{-2}} \tag{17}$$

that with $R = K$ leads to realization

$$H_{\mathrm{s}}(z) = 0.5 \frac{q_1 + (q_2 + 1) z^{-1}}{1 + 0.5 q_1 z^{-1} + 0.5 (q_2 - 1) z^{-2}} z^{-1} \tag{18}$$

4. WAVE DIGITAL BELL

As a W-modeling case using modal decomposition, a 'semiphysical' driving point impedance of a bell is investigated next. In earlier papers we have studied sound synthesis of bells using inharmonic digital waveguides and modal filterbanks [12, 13]. High-resolution analysis of modal data was achieved using the frequency-zooming ARMA analysis (FZ-ARMA) technique as developed in [14]. This is able to resolve for each partial a set of modes, very close in frequency, which produce the beating inherent in typical bell sounds.

Real bells are physical objects that, as 3-D structures, have an inharmonic set of partials [1]. By proper tuning several of the lower partials can be made approximately harmonic, but there always remains at least one perceptually important inharmonic component. In untuned small handbells there may not be any harmonic structure. Slight asymmetries are the reason to partials as mode groups and the perceivable beating (warble).

In a detailed model of a real bell the modal decomposition should describe the spatial distribution of modal shapes so that a force excitation in any point could be solved for the spatial distribution of the exponentially decaying modes as well as for the sound radiated from bell surfaces. Instead we in this paper develop a wave digital model based on modal decomposition that considers the bell only as a driving point impedance with related force and velocity. We may calibrate such a semiphysical model simply according to a sound recording of an existing bell and realize a model that sounds realistic, being efficient for real-time synthesis.

Table 1: *Modal data for the bell of the case study including two modes per partial: mode frequencies (f_1 and f_2), initial amplitudes (A_1 and A_2), and decay time constants (τ_1 and τ_2) are given.*

n	f_1/Hz	τ_1/s	A_1	f_2/Hz	τ_2/s	A_2
1	850.8	0.165	0.0723	851.3	0.749	0.0965
2	1702.3	0.464	0.1497	1703.1	0.421	0.0514
3	2026.7	0.355	0.1258	2032.8	0.048	0.0734
4	2787.2	0.131	0.0763	2792.5	0.079	0.0364
5	3404.7	0.251	0.0610	3407.0	0.098	0.0716
6	4552.1	0.028	0.0290	4559.6	0.110	0.0278
7	4889.6	0.149	0.0554	5050.5	0.259	0.0511
8	6881.5	0.149	0.1261	6889.2	0.051	0.0088
9	8549.8	0.153	0.0029	8631.9	0.023	0.0047
10	8695.0	0.109	0.0313	8842.0	0.153	0.0191

We have taken a particular bell and analyze its prominent modal components using the FZ-ARMA analysis. Table 1 lists the modal data from a bell recording[2]. Two modes are fitted to each partial below 10 kHz to realize proper beating for the partials.

For a wave-based modeling we may use the analyzed modal data by constructing a wave port with a corresponding driving-point impedance. The task is now to construct a port compatible with W-modeling that implements a driving point impedance so that when the bell is hit by a proper hammer-like object (force excitation), it makes a desired sound (port velocity as output).

There are several ways to construct the port impedance of interest, for example:

1. Make the modes by basic WDF components as series resonators, as shown in Fig. 2. Pairs of modes are then combined in parallel into partials, which are further connected in parallel to make a full port impedance.
2. Implement each mode or a mode group for a partial as a filter structure according to the rules described in Section 3.3, and connect the partials in parallel.
3. Realize the whole impedance, composed of all modes, as a single filter, according to Eq. (16).

It is obvious that progressing from case 1 to 3 the computational efficiency of implementation can be improved, since consolidating functionality can utilize the advantages of DSP more than composing a model from lumped WDF elements. Case 2 benefits from the possibility of controlling the properties of each mode separately, while in case 3 only the composite filter coefficients are directly accessible. In case 1 the equivalent lumped components, corresponding in some way to masses, spring constants and damping factors, are directly controllable.

One particular design issue with case 1 is the bilinear mapping when creating reactances with WDFs. The formulas of reference resistance for capacitance C and inductance L in electrical circuits are:

$$R_{\mathrm{C}} = 1/2Cf_s \quad \text{and} \quad R_{\mathrm{L}} = 2Lf_s \tag{19}$$

where R_{C} and R_{L} are the related WDF port resistances and f_s is the sample rate. However, due to the bilinear mapping between

[2]This is a relatively high-pitch bell from the Belfort bell recordings, provided by Mark Leman.

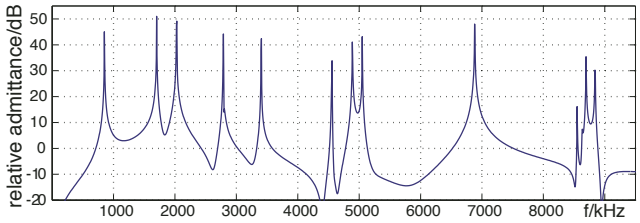

Figure 5: *Synthesized bell port admittance function.*

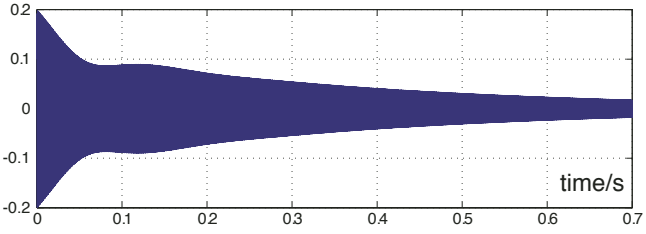

Figure 6: *Temporal envelope of the third partial.*

analog angle frequency $\omega = 2\pi f$ and discrete-time angle frequency Ω by

$$\omega = g(\Omega) = (2/T_s)\tan(\Omega T_s/2) \tag{20}$$

the frequency scale is warped [3] so that while $\Omega \to f_s/2$, the corresponding analog angle frequency $\omega \to \infty$. Thus the inductances and capacitances in a WDF realization have to be prewarped to get correct modal frequencies and decay times. In cases 2 and 3 above the filter design process takes automatically care of proper frequencies and decay rates. In each case 1–3 the wave digital port realized is functionally equivalent.

Figure 5 shows the admittance function (dB scaled) of the port implemented from data in Table 1, and Fig. 6 plots the temporal envelope of partial number 3 showing beating in decay.

To make a full bell model with a hammer striking the driving point, the hammer has also to be modeled. The contact is a nonlinear (time-varying) one, thus special techniques are needed to make it energetically correctly to guarantee stability. There are two principles available to this: using power-normalized waves discussed above (see also [15]) or by nonlinear reactance through mutator type of adaptor [2]. These techniques allow for complex nonlinear contact of the hammer and the bell as it happens also with the piano hammer [15].

The WDF bell with impulsive hit sounds different from the recording used for calibration for two reasons. First, the attack needs a more complex bell model for more realistic sound, and secondly, reverberation and reflections of the space surrounding the bell. In other aspects the timbre is very realistic, including correct type of beating and decay envelope.

5. DISTRIBUTED NONLINEARITIES BY DWG'S

Distributed nonlinearities are among the most challenging tasks in physics-based modeling. They are quite common in musical instruments, although in many cases a linearized model is a useful approximation. In this Section we investigate how the tension modulation nonlinearity in strings can be realized through digital waveguide principles.

When a real string is displaced, it is elongated causing an increase in its tension and thus also in its fundamental frequency. The elongation of the string can be expressed as [16]

$$l_{\rm dev}(t) = \int_0^{l_{\rm nom}} \sqrt{1 + (y_x(t,x))^2}\,dx - l_{\rm nom} \tag{21}$$

where l_{nom} is the nominal string length, x is the spatial coordinate along the string, and y is the displacement of the string. Note, that since the elongation calculation is done globally, i.e. for the whole string in one piece, we lose the information concerning local elongations and effectively consider the tension as being uniform for the whole string. In real strings this is not the case, although longitudinal waves do propagate considerably faster than the transversal ones. The elongation can be approximated for the digital waveguide as [17]

$$L_{\rm dev}(n) \approx \frac{1}{2}\sum_{m=0}^{\hat{L}_{\rm nom}} [s_{\rm r}(n,m) + s_{\rm l}(n,m)]^2 \tag{22}$$

where $s_{\rm r}(n,m)$ and $s_{\rm l}(n,m)$ are the slope waves at time instant n and position m, propagating right and left, respectively, and $\hat{L}_{\rm nom}$ is the rounded nominal string length.

Since the transversal wave propagation velocity is proportional to the string tension, the change in tension corresponds to a change in the wave velocities. In DWGs this can be implemented by modulating the delay line lengths. This is done by inserting first-order allpass filters between each unit delay in the delay line and then varying the allpass-filter coefficients. This is illustrated in Fig. 7. The excitation to the string can be inserted during run-time as a force signal using an interaction block, denoted by I. This block is essentially a 3-port parallel junction of Fig. 1, with the third port omitted and the excitation signal used as an external force.

The first-order allpass filter is of the form

$$A(z) = \frac{-a + z^{-1}}{1 - az^{-1}} \tag{23}$$

where a is the filter coefficient which defines the length of the delay caused by the filter. The approximated delay for each allpass filter can be expressed as [17], [18]

$$d_{\rm ap}(n) \approx -\frac{1}{2N}\sum_{l=n-1-\hat{L}_{\rm nom}}^{n-1} (1 + \frac{EA}{K_0})\frac{L_{\rm dev}(l)}{L_{\rm nom}} \tag{24}$$

where E is Young's modulus, A is the cross-sectional area of the string, and K_0 is the nominal tension corresponding to the string at rest. N denotes the total number of allpass filters in the structure. The allpass-filter coefficient a can now be written as

$$a = (1 - d_{\rm ap})/(1 + d_{\rm ap}). \tag{25}$$

It is important to note that the string model presented in Fig. 7 simulates a string vibrating in one polarization only. For a more realistic model, another such structure should be used for modeling the second polarization. This is especially true in the case of the *kantele*, a traditional Finnish plucked-string instrument, where the two vibration polarizations have different effective lengths due to a knotted termination of the string [19]. Using two nonlinear DWG string models with slightly different lengths, a synthesis model of the kantele can be generated. For a more thorough discussion of the kantele model and the nonlinear DWG string, see [18].

The synthesis results reveal that the initial pitch glide phenomenon can be realistically modeled using the nonlinear DWG string. The fundamental frequencies of a real kantele recording and the synthesized tone are illustrated in Figure 8.

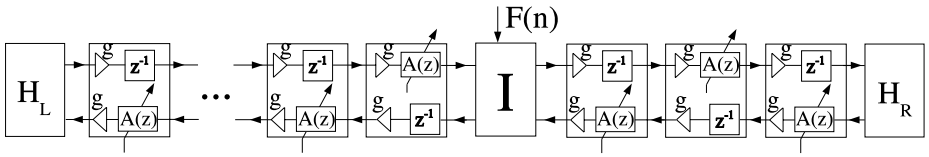

Figure 7: *A nonlinear DWG string. The string consists of allpass filters, denoted $A(z)$, connected via unit delays for avoiding delay-free loops. H_L and H_R denote loop filters simulating the frequency-dependent losses and g is a scaling coefficient for modeling frequency-independent losses. $F(n)$ represents the excitation force signal applied on the string.*

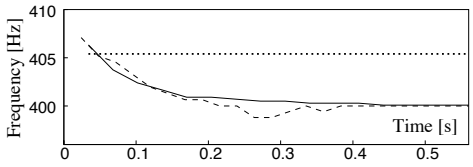

Figure 8: *Illustration of the fundamental frequency glide in the synthesized tone (solid line) and in a real kantele tone, obtained via measurements (dashed line). The approximated detection threshold of a pitch drift [20], illustrated as a dotted line, suggests that the fundamental frequency drifts in both cases are audible.*

The generation of missing harmonics can also be simulated, if the boxcar integration of Eq. (24) is replaced with a leaky integrator, as suggested in [17]. Then, the leaky integrator parameters can be used to control the amplitudes of the missing harmonics. Note that this solution is not physics-based, since the error in the integration creates the mode-coupling, but it still is an efficient way of emulating the phenomenon.

6. SUMMARY

In this paper we have presented recent results from the HUT Sound Source Modeling group. A theoretical discussion covered different discrete-time modeling paradigms, divided in W- and K-modeling approaches, their interrelationships, and how they can be combined. Two particular cases have been described: a wave digital bell based on modal decomposition of a port impedance and distributed nonlinearity modeling by digital waveguides.

7. ACKNOWLEDGEMENTS

This work is supported by the IST/ALMA project (ALgorithms for the Modelling of Acoustic interactions, IST-2001-33059) and the Academy of Finland project SA 53537. Paulo Esquef has been supported by the Brazilian National Council for Scientific and Technological Development (CNPq).

8. REFERENCES

[1] N. H. Fletcher and T. D. Rossing, *The Physics of Musical Instruments*, Springer-Verlag, New York, 1991.

[2] A. Sarti and G. de Poli, "Towards Nonlinear Wave Digital Filters," *IEEE Trans. on Sig. Proc.*, vol. 47, no. 6, pp. 1654–1668, June 1999.

[3] A. Fettweis, "Wave Digital Filters: Theory and Practice," *Proc. of the IEEE*, vol. 74, no. 2, pp. 270–361, Feb. 1986.

[4] Julius O. Smith, *Principles of Digital Waveguide Models of Musical Instruments*, Chapter 10 in *Applications of Digital Signal Processing to Audio and Acoustics*, (ed. Kahrs and Brandenburg), Kluwer Academic Publishers, 1998.

[5] S. D. Bilbao, *Wave and Scattering Methods for the Numerical Integration of Partial Differential Equations*, PhD Thesis, Stanford University, May, 2001.

[6] J. Strikwerda, *Finite Difference Schemes and Partial Differential Equations*, Wadsworth and Brooks, Grove, Ca, 1989.

[7] A. Chaigne, "On the Use of Finite Differences for Musical Synthesis. Application to Plucked Stringed Instruments," *J. Acoustique*, vol. 5, pp. 181–211, April 1992.

[8] M. Karjalainen and C. Erkut, "Digital Waveguides vs. Finite Difference Schemes: Equivalance and Mixed Modeling," *J. Applied Sig. Proc.*, no. 7, 2004, pp. 978–989.

[9] J.-M. Adrien, *The Missing Link: Modal Synthesis*, chapter in *Representations of Musical Signals*, (eds. de Poli, Piccialli, and Roads), MIT Press, Cambridge, Mass., 1991.

[10] L. Trautmann, *Digital Sound Synthesis by Physical Modeling of Musical Instruments Using Functional Transformation Methods*, PhD Thesis, Univ. Erlangen-Nürnberg, Germany, 2002.

[11] M. Karjalainen, "1-D digital Waveguide Modeling for Improved Sound Synthesis," in *Proc. IEEE ICASSP'02*, Orlando, May 2002, pp. 1869–1872.

[12] M. Karjalainen, P. A.A. Esquef, and V. Välimäki, "Efficient Modeling and Synthesis of Bell-Like Sounds," in *Proc. DAFx'02*, Hamburg, Germany, Sept. 2002, pp. 181–186.

[13] M. Karjalainen, V. Välimäki, and Paulo A.A. Esquef, "Making of a Computer Carillon," in *Proc. SMAC'03*, Stockholm, Sweden, Aug. 2003, pp. 181–186.

[14] M. Karjalainen, P. A. A. Esquef, P. Antsalo, A. Mäkivirta, and V. Välimäki, "Frequency-Zooming ARMA Modeling of Resonant and Reverberant Systems," *J. Audio Eng. Soc.*, vol. 50, no. 12, pp. 1012–1029, Dec. 2002.

[15] J. Bensa, S. Bilbao, R. Kronland-Martinet, and J. O. Smith, "A Power Normalized Non-Linear Lossy Piano Hammer," in *Proc. SMAC'2003*, Stockholm, Sweden, 2003, pp. 365–368.

[16] K. A. Legge and N. H. Fletcher, "Nonlinear generation of missing modes on a vibrating string," *J. Acoust. Soc. Am.*, vol. 76, pp. 5–12, July 1984.

[17] T. Tolonen, V. Välimäki, and M. Karjalainen, "Modeling of tension modulation nonlinearity in plucked strings," *IEEE Trans. SAP*, vol. 8, no. 3, pp. 300–310, May 2000.

[18] J. Pakarinen, M. Karjalainen, and V. Välimäki, "Modeling and real-time synthesis of the kantele using distributed tension modulation," in *Proc. SMAC'03*, Stockholm, Sweden, August 6-9, 2003, vol. 1, pp. 409–412.

[19] C. Erkut, M. Karjalainen, P. Huang, and V. Välimäki, "Acoustical analysis and model-based sound synthesis of the kantele," *JASA*, vol. 112, pp. 1681–1691, October 2002.

[20] H. Järveläinen and V. Välimäki, "Audibility of initial pitch glides in string instrument sounds," in *ICMC'2001*, Havana, Cuba, 17-23 September 2001, pp. 282–285.